Influence of the pulse shape and the dot size on the decay and reappearance of Rabi rotations in laser driven quantum dots

M. Glässl,[1,*] M. D. Croitoru,[1] A. Vagov,[1] V. M. Axt,[1] and T. Kuhn[2]
[1]*Institut für Theoretische Physik III, Universität Bayreuth, DE-95440 Bayreuth, Germany*
[2]*Institut für Festkörpertheorie, Westfälische Wilhelms-Universität Münster, Germany*
(Received 11 February 2011; revised manuscript received 27 July 2011; published 7 September 2011)

We study the dynamics of strongly confined semiconductor quantum dots coupled to acoustic phonons and driven by external laser pulses by a numerical path integral method. The field-dependent damping, caused by the non-Markovian processes of pure dephasing and manifesting itself in the peculiar decay and reappearance phenomenon of Rabi rotations is found to depend notably on the dot size and the shape of the applied laser pulses. In the limit of strong fields rectangular pulses yield a significant weaker damping than Gaussian or other bell-shaped profiles. As a consequence, the undamping of Rabi rotations at high pulse areas is most clearly visible for rectangular pulses.

DOI: 10.1103/PhysRevB.84.125304 PACS number(s): 03.65.Yz, 73.63.Kv, 42.50.Md, 63.20.kk

I. INTRODUCTION

The ability of integration in solid-state devices together with the possibility of designing tailored spectra make quantum dots (QDs) very attractive for the realization of quantum information processing devices.[1] Many proposals for quantum information applications in a solid-state environment base upon the idea to manipulate localized excitonic states in a controlled way by applying ultrafast laser pulses.[2–6] A key ingredient of all these schemes is the manipulation by means of Rabi oscillations (ROs). As the occupations as a function of time are often difficult to measure, many experiments investigate Rabi rotations (RRs) instead of ROs, i.e., the final exciton occupation is recorded as a function of the applied pulse area.[7–10]

The major obstacle to deal with when realizing those proposals is decoherence, arising from the unavoidable coupling of the electronic system to the environment. If semiconductor quantum dots are used as building blocks in quantum information theory, a detailed knowledge of the dephasing processes present in these systems is of utmost importance in order to be able to face this challenge. In the limit of strong electronic confinement the energetically large separation between different electronic levels justifies the restriction to only two levels, and the contribution of phonon-assisted virtual transitions, which do not change the electronic occupation, provides the dominant dephasing mechanism on a picosecond time scale.[11,12] This holds for temperatures up to ~ 100 K, where other dephasing mechanisms such as radiative decay evolve on much longer time scales.[13] The virtual processes, usually referred to as pure dephasing, can be regarded as a prototype of a genuine non-Markovian interaction and give rise to several interesting features, such as a phonon-induced renormalization of the Rabi frequency,[14–16] a nonmonotonic temperature dependence of the initial decay,[12] or strongly non-Lorentzian line shapes in photoluminescence spectra.[17,18] Experimental data are in excellent quantitative agreement with these theoretical predictions[12] and clearly confirm that even at $T = 100$ K in typical self-assembled QDs the initial decoherence is dominated by pure dephasing processes.

Using a numerically exact path integral method[19–23] we have shown recently that the phonon-induced damping of ROs, which manifests itself in a damping of RRs and thus limits the fidelity in the control of electronic excitations in QDs, is a nonmonotonic function of the applied laser field.[15,24] In the limit of weak fields the damping increases with rising field strengths, while it decreases at high fields. This nonmonotonic behavior, which can be understood as a resonance phenomenon[25] and occurs for all temperatures and carrier-phonon coupling strengths, therefore results in a peculiar reappearance of RRs at strong fields. We would like to stress that this reappearance of RRs is different from the collapse and revival phenomenon within the Jaynes-Cummings model,[26] which describes the temporally periodic modulation of ROs in a two-level system coupled to a single-mode quantized photon field.

Recent progress in experimental techniques[10] provided access to higher values of the pulse area, which is a prerequisite for the observation of the reappearance of RRs in the experiment. It has been demonstrated that the period of RRs decreases with the pulse area and increases with rising values of the temperature, which is consistent with theoretical calculations.[15,24] Moreover, these experiments gave some first evidence for the predicted onset of the reappearance of RRs at high pulse areas.

In this work we characterize the dependence of the decay and reappearance phenomenon on the dot size and the shape of externally applied laser pulses, comparing results for rectangular, Gaussian, and sech-shaped pulses. As elaborated below, both dependencies strongly affect the system dynamics. In particular, a proper choice of the pulse envelope function can lead to a reduction of the dephasing. Our studies may be helpful to support the interpretation of experimental data as well as to guide further experimental work. Namely, we identify parameter regions which are favorable to observe the decay and reappearance phenomenon experimentally. In addition, we deepen our knowledge about phonon-induced damping of ROs and the corresponding renormalization of the Rabi frequency, which is important for constructing quantum information schemes that rely on controlled excitonic excitations.

The paper is organized as follows. In Sec. II we briefly introduce the model. The influence of both the dot size and the pulse shape on the field-dependent damping is presented in detail in Sec. III. Finally, we summarize our results in Sec. IV.

II. MODEL

We consider a GaAs QD in the strong confinement limit modeled by an electronic two-level system coupled to an external laser field and to a continuum of acoustic phonons, and concentrate on pure dephasing processes. This allows us to use the well-known two-level independent boson (TLIB) model:[11,27]

$$\widehat{H} = \hbar\frac{\Omega}{2}(\widehat{1}-\widehat{\sigma}_z) + \frac{\hbar}{2}(\widehat{1}-\widehat{\sigma}_z)\sum_{\mathbf{q}}\left(\gamma_{\mathbf{q}}b_{\mathbf{q}}^{\dagger}+\gamma_{\mathbf{q}}^{*}b_{\mathbf{q}}\right) + \hbar\sum_{\mathbf{q}}\omega_{\mathbf{q}}b_{\mathbf{q}}^{\dagger}b_{\mathbf{q}} - \mathbf{d}\mathbf{E}(t)\widehat{\sigma}_{-} - \mathbf{d}^{*}\mathbf{E}^{*}(t)\widehat{\sigma}_{+}. \quad (1)$$

Here $\widehat{\sigma}_{\pm} = \widehat{\sigma}_x \pm i\widehat{\sigma}_y$, where $\widehat{\sigma}_x$, $\widehat{\sigma}_y$, and $\widehat{\sigma}_z$ denote Pauli matrices acting on the electronic space, Ω defines the energy gap between the two QD states, and $b_{\mathbf{q}}^{\dagger}$ ($b_{\mathbf{q}}$) are bosonic creation (annihilation) operators of a phonon with momentum $\mathbf{q}$ and energy $\hbar\omega_{\mathbf{q}}$. The interaction with the classical light field $\mathbf{E}$ is treated in the usual dipole and rotating wave approximation and takes the form $\mathbf{dE}(t) = \frac{\hbar}{2}f(t)e^{-i\widetilde{\Omega}t}$ with a real envelope function $f(t)$ representing the instantaneous Rabi frequency and the laser frequency $\widetilde{\Omega}$ being in resonance with the polaron-shifted exciton transition. For brevity, we shall refer to f as the field strength in the following. We assume that the electric field is circularly polarized. This leads to the creation of excitons in a circularly polarized state and justifies the restriction to a two-level system by preventing the generation of biexcitons.[28] The coupling to phonons is only present if the system is in its upper state and characterized by the exciton-phonon coupling constants $\gamma_{\mathbf{q}} = \gamma_{\mathbf{q}}^{e} - \gamma_{\mathbf{q}}^{h}$, which are given as the difference between the electron-phonon and the hole-phonon coupling constants. Assuming that the dot and the surrounding barrier material do not differ significantly in their lattice and dielectric properties, the phonon modes can be approximated by three-dimensional bulk modes and the coupling constants separate into two factors,[18]

$$\gamma_{\mathbf{q}}^{e(h)} = \Psi^{e(h)}(\mathbf{q})\, G_{\mathbf{q}}^{e(h)}. \quad (2)$$

The form factor $\Psi^{e(h)}$ is defined as the Fourier transformation of the square modulus of the carrier wave functions. For simplicity, we consider spherical dots with wave functions given by the ground state solution of a harmonic potential, yielding

$$\Psi^{e(h)}(\mathbf{q}) = \exp\left(-\mathbf{q}^2 a_{e(h)}^2/4\right), \quad (3)$$

where $a_{e(h)}$ represents the electron (hole) geometrical confinement. In the following, we will refer to the quantity $a := a_e$ as the dot size and set $a_h = 0.87\,a$. The second factor in the coupling constants, $G_{\mathbf{q}}^{e(h)}$, depends on the specific coupling type. As for GaAs self-assembled QDs the deformation potential coupling to LA phonons provides by far the largest contribution to pure dephasing we concentrate on this mechanism. The explicit form of $G_{\mathbf{q}}^{e(h)}$ for this case can be found in Ref. 18.

III. RESULTS

The theory described so far is used to study the influence of varying dot sizes and different pulse shapes on the time evolution of the electronic system. To obtain these results we use a numerically exact real-time path integral method.[19–23] Recently, this elaborate scheme was compared to more widely used methods invoking perturbative and Born-Markov approximations.[22,29] Although approximate methods yield trustable results for a certain range of parameters,[9,10] pronounced quantitative and even qualitative differences were found in the cases of strong coupling or high temperatures.[29] A detailed description of our algorithm analyzing both the necessary physical requirements as well as the actual implementation is presented in Ref. 19.

As previously shown in Ref. 24, for rectangular pulses the exciton occupation experiences a phonon-induced damping which is a nonmonotonic function of the applied field strength. The maximal dephasing occurs if the Rabi frequency is in resonance with the frequency of the most strongly coupled phonons. Note that a stronger damping in the time domain corresponds to weaker oscillations at long times and translates into a stronger reduction of the amplitude of RRs. Hence, the nonmonotonic dependence of the damping on the laser intensity leads to an undamping of RRs at high pulse areas. Here, we analyze how this interesting phenomenon, and therefore, the field-dependent damping changes by varying the dot size or using differently shaped pulses.

A. Dependence on the dot size

Let us first concentrate on the influence of the dot size. Figure 1 shows the exciton occupation after excitation with rectangular pulses of 20 ps duration for different temperatures and dot sizes as a function of the pulse area

$$A = \int_{-\infty}^{\infty} f(t)\,dt, \quad (4)$$

given as the total rotational angle in the phonon-free dynamics. With decreasing dot size a the field-dependent damping reflected in the reduction of the amplitude of RRs is considerably enhanced: The maximal reduction taking place at a critical pulse area $A = A_c$ becomes stronger, and the region with likewise strong damping increases as well. In addition, the critical pulse area rises significantly with smaller width of the electronic confinement.

The enhancement of the dephasing for reduced dot sizes can be explained easily by means of the coupling constants as given in Eq. (2): With decreasing size of the QD, the form factors $\Psi^{e(h)}$ entering these coupling constants extend to higher q values. Probing a considerably wider range of frequencies contained in the continuum of acoustic phonons, the dephasing in small QDs is significantly enhanced. This leads to a stronger damping of ROs during the evolution in time, which is reflected in a stronger reduction of the amplitude of RRs.

For arbitrary pulse shapes, the dynamics of the TLIB model may be quite involved. However, it turned out that for

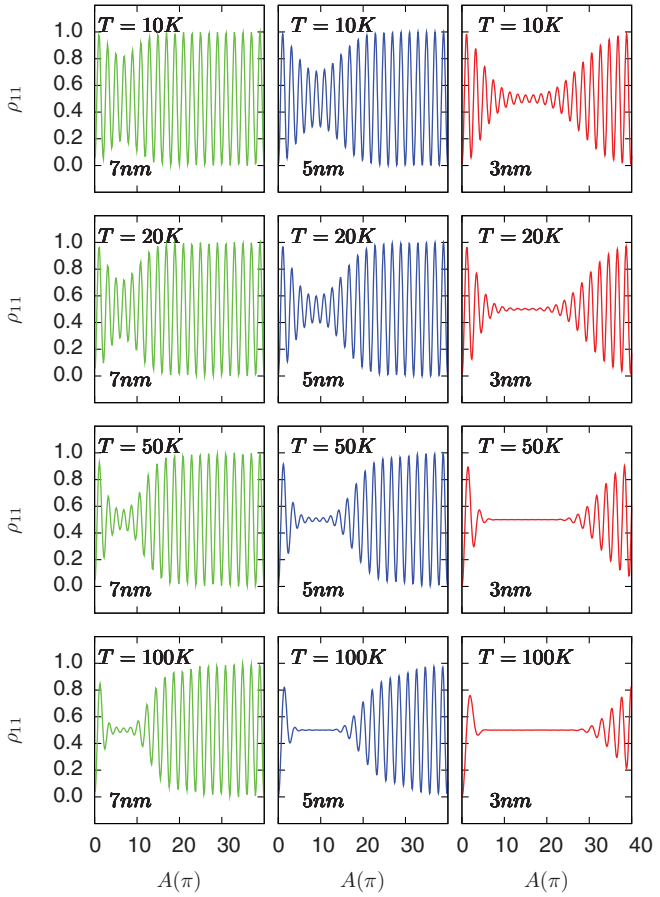

FIG. 1. (Color online) Quantum dot occupation after excitation with rectangular pulses of 20 ps duration as a function of the pulse area A at different temperatures and for dot sizes of $a = 7$ nm (left), $a = 5$ nm (middle), and $a = 3$ nm (right).

excitations with rectangular pulses, the time dependence of the exciton occupation during the pulse can be approximated by the simple exponential expression[15]

$$\rho_{11} = \tfrac{1}{2}[1 - \cos(\omega t)\exp(-\gamma_d t)], \tag{5}$$

that allows one to extract both the effective damping rate γ_d of ROs as well as their frequency ω by fitting the numerical data. In Fig. 2 we concentrate on this case and show the damping constant γ_d at $T = 10$ K and $T = 100$ K for dots of 3 nm (red solid), 5 nm (blue dashed), and 7 nm (green dotted) size as a function of the field strength f, which in the case of rectangular pulses is given as the quotient of the pulse area and the pulse duration. In our calculations, we fixed the pulse duration to 20 ps and varied the pulse area. However, fixing the latter and varying the pulse length leads to identical results, as the damping rate (as well as the frequency ω) is solely determined by f. It should be noted that this contrasts to the results in Fig. 1, which significantly depend on the pulse length, as shown below. The main differences already discussed for the decay and reappearance of RRs in Fig. 1 become apparent. For decreasing dot sizes, the maximal damping increases, the region with pronounced damping becomes larger, and the critical field strength is shifted to higher values. As commonly expected, rising temperatures strongly enhance the

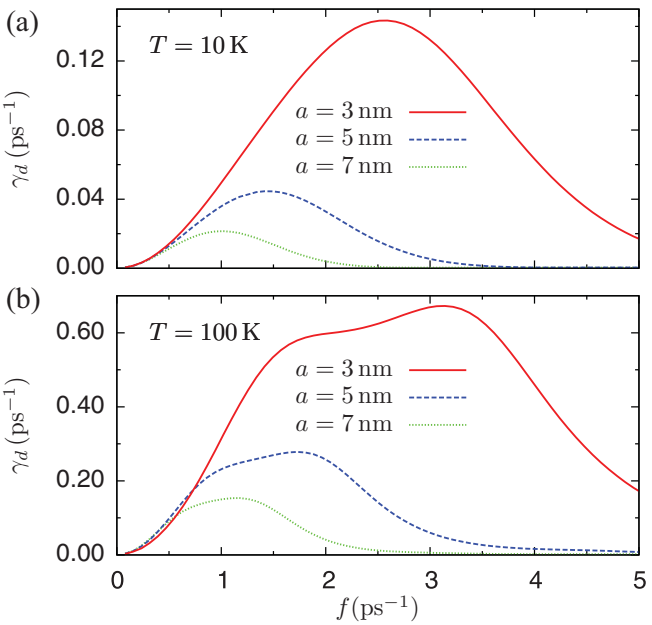

FIG. 2. (Color online) Damping rate γ_d as a function of the field strength f at (a) $T = 10$ K and (b) $T = 100$ K for different dot sizes.

damping. Interestingly, for weak fields the damping is almost independent on the dot size for all temperatures.

As explained in Refs. 15 and 24 and already mentioned above, the damping is dominated by the most strongly coupled phonons having wavelengths comparable to the quantum dot size. It turns out that the critical field strength f_c, defined as the field strength with maximal damping, can roughly be approximated by $f_c = 2\pi/\tau$, where τ is the flight time of a phonon through the dot. As the time a phonon needs to pass the dot decreases with decreasing dot size, the shift of the maximal damping to higher values of the field strength can intuitively be understood.

Considering small values of the field strength below $f = 0.5$ ps^{-1}, the damping is approximately independent on the dot size. However, in this parameter range the normalized frequency $\omega_{\text{norm}} = \omega/f$, defined as the ratio between the frequency ω of ROs and the phonon-free Rabi frequency f, shows a pronounced dependence on the dot size. The extracted values of ω_{norm} as a function of f are presented in Fig. 3. For all dot sizes, the normalized frequency shows a nonmonotonic behavior, being considerably smaller than 1 for weak fields, exceeding unity at intermediate fields, and reaching the value $\omega_{\text{norm}} = 1$ in the strong-field limit. This behavior is more pronounced for both higher temperatures and decreasing dot sizes. For a 3-nm-sized QD at $T = 100$ K and for field strengths tending to zero, the normalized frequency drops down to 0.44 leading to a normalized period which exceeds the phonon-free period by more than a factor of 2 [cf. Fig. 3(a)]. As a consequence an applied 2π pulse with a small field strength will not even provide full inversion instead of a complete Rabi flop, which would be expected in the phonon-free case. These strong deviations from what one would expect when thinking about the limiting case of a two-level system without dephasing due to phonons may be important for many proposals for quantum information

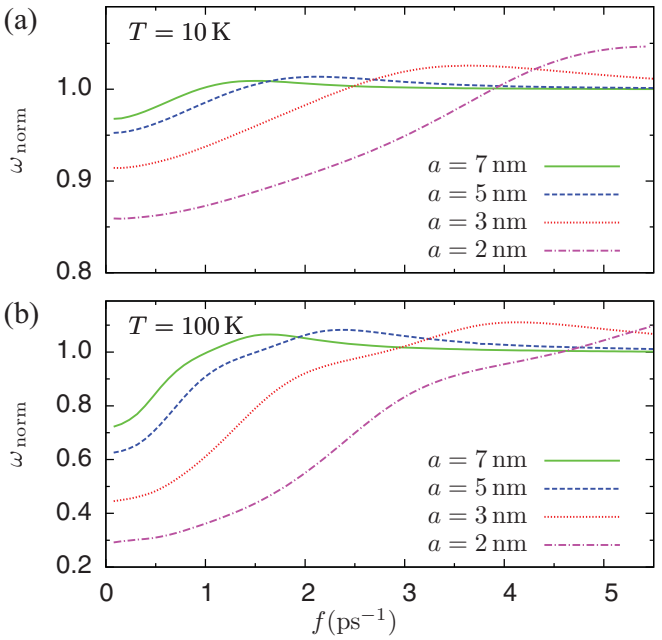

FIG. 3. (Color online) Normalized frequency $\omega_{\rm norm}$, defined as the ratio of the Rabi frequencies with and without phonons, as a function of the applied field strength at temperatures of (a) $T = 10$ K and (b) $T = 100$ K for different dot sizes.

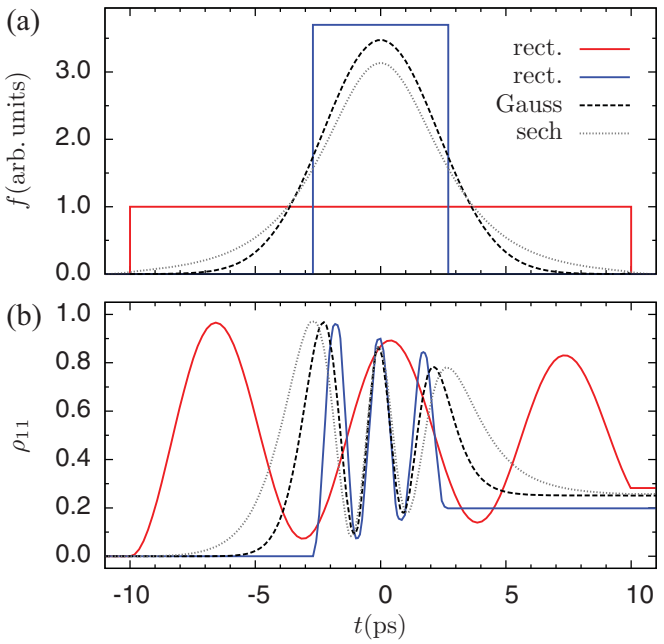

FIG. 4. (Color online) (a) Envelope functions $f(t)$ for rectangular pulses of 20 and 5.4 ps duration, a Gaussian pulse, and a sech-shaped pulse having identical pulse areas. The full width at half maximum for both the Gaussian and the sech-shaped pulse is 5.4 ps. (b) ROs of a 3-nm-sized QD, driven by the four pulses introduced in (a) for $A = 6\pi$ and at $T = 1$ K.

applications in a solid-state environment that rely on the controlled manipulation of localized excitonic states in QDs by using ROs.[2–4,6] For a 2-nm-sized dot the normalized frequency is further decreased for a wide range of field strengths, falling below 0.3 in the weak-field limit. We would like to stress that for smaller dots the model presented in this work becomes questionable as it is not possible to localize electronic wave functions in an arbitrarily small dot.

B. Dependence on the pulse shape

Let us now turn to the influence of the pulse shape $f(t)$. Besides rectangular pulses with $f(t) = \text{const}$, which are often used due to their simplicity, we investigate more realistic profiles, namely, Gaussian and sech-shaped ones, naturally provided by many laser sources. In contrast, rectangular pulses are to some extent artificial but they can, in principle, be realized applying well-known pulse-shaping techniques.[30] For our calculations, we choose the full width at half maximum (FWHM) of the Gaussian and sech-shaped pulses to be 5.4 ps and compare pulses having the same pulse area. However, this condition does not fix the length of the rectangular pulse. Therefore, we consider two different rectangular pulses with durations of $\tau = 5.4$ and 20 ps, respectively: Choosing $\tau = 5.4$ ps, the length of the rectangular pulse conincides with the FWHM of the Gaussian and sech-shaped pulses, whereas for $\tau = 20$ ps, the envelope functions of both bell-shaped pulses are localized in the time interval given by the rectangular pulse, yielding another interesting comparison. All four profiles are displayed in Fig. 4(a).

Figure 4(b) shows ROs of a 3-nm-sized QD at $T = 1$ K for the four pulses presented in Fig. 4(a) and a pulse area of $A = 6\pi$. Independent on the pulse shape, the system shows three Rabi flops. The temporal evolution, however, depends significantly on the chosen profile. In the case of rectangular pulses the excitonic occupation oscillates with a fixed frequency. Contrarily, the occupation oscillates with a temporally varying frequency for Gaussian or sech-shaped pulses as the strength of the optical driving is here time dependent. For times near the pulse maximum at $t = 0$ the field strengths of both bell-shaped pulses exceed the constant field strength of the 20 ps lasting rectangular pulse by far, and therefore, the system dynamics develops much faster, but still slower than for the 5.4 ps lasting rectangular pulse with an even larger field strength. Note that according to Eq. (1), the exciton occupation can only change as long as a laser pulse is applied. For rectangular pulses with an unsteady envelope this leads to a kink in the occupation when the laser is switched off.

In the following, we will demonstrate that the choice of the pulse shape considerably affects the decay and reappearance of RRs and concentrate first on the case where the length of the rectangular pulse coincides with the FWHM of the Gaussian and the sech-shaped pulse. To this end, we calculated RRs at $T = 10$ and 100 K using rectangular, Gaussian, and sech-shaped pulses of 5.4 ps duration. For QDs of 5 and 3 nm size, the results are shown in Figs. 5(a) and 5(b), respectively. As the differences between Gaussian and sech-shaped pulses are less pronounced, we will first discuss rectangular and Gaussian profiles and comment later on sech-shaped ones.

Comparing the decay and reappearance phenomenon of RRs for the Gaussian pulse with respect to the rectangular pulse, we find two main differences: (i) The minimal amplitude is shifted to higher pulse areas, causing a later onset of the

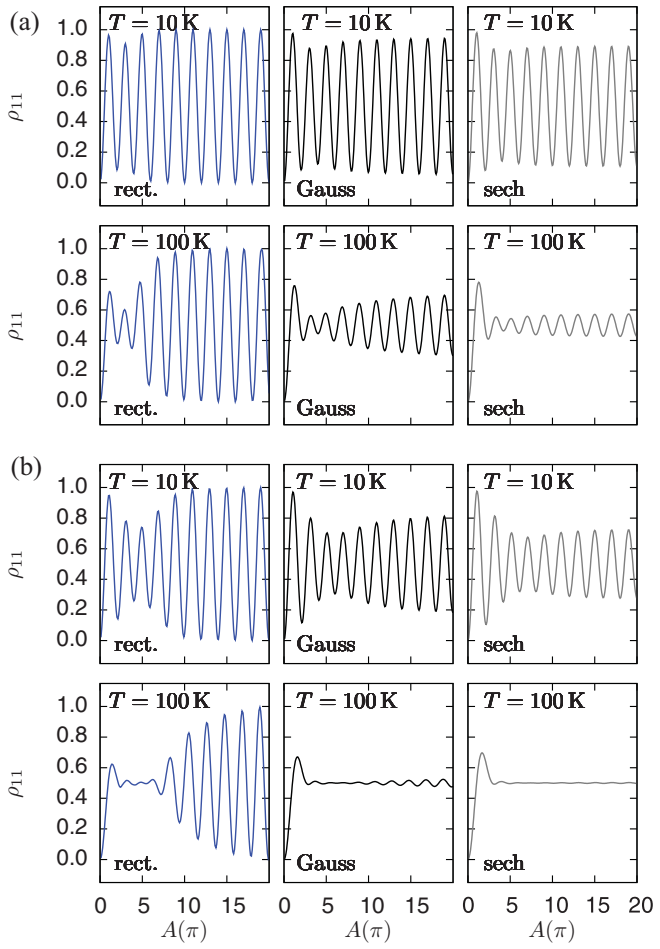

FIG. 5. (Color online) Quantum dot occupation after excitation with rectangular, Gaussian, or sech-shaped pulses (duration/FWHM: 5.4 ps) as a function of the pulse area A at $T = 10$ K and $T = 100$ K for a dot of (a) $a = 5$ nm and (b) $a = 3$ nm size.

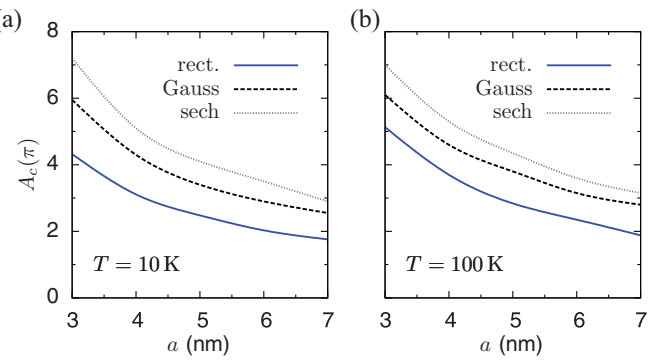

FIG. 6. (Color online) Pulse area with maximal damping A_c as a function of the dot size a for rectangular, Gaussian, and sech-shaped pulses (duration/FWHM: 5.4 ps) at temperatures of (a) $T = 10$ K and (b) $T = 100$ K.

reappearance. (ii) At high pulse areas the damping is stronger and, most important, the reappearance rate is significantly reduced, i.e., the increase of the amplitude of RRs as a function of the pulse area is less. Thus, the decay and reappearance is more clearly visible for rectangular pulses. The physical reason underlying these differences is that unlike rectangular pulses, Gaussian pulses contain a broad interval of instantaneous field strengths that are smaller than (in the tails) or at most similar to (in the peak region) the constant field strength of a rectangular pulse with equal pulse area [cf. Fig. 4(a)]. This leads to components with reduced or enhanced damping, and the differences specified above can be explained as follows.

In the limit of weak fields, $f < f_c$, the field strengths contained within the Gaussian pulse correspond to smaller damping rates than the rate belonging to the rectangular pulse (cf. Fig. 2). This implies that for the Gaussian pulse, higher pulse areas have to be applied to reach the strongest damping, and thus, the critical pulse area A_c is shifted to higher values. In Fig. 6 this shift is presented as a function of the dot size. As seen in Fig. 4(b), for a Gaussian pulse the electronic occupation oscillates with a frequency varying with time, and therefore, it is not possible to extract the damping rate γ_d via fitting the numerical solution with Eq. (5). Nevertheless, the pulse area with maximal damping can easily be determined from the extrema of the envelope functions of RRs (cf. Fig. 5). Due to the fact that a Gaussian pulse contains a wide range of field strengths, its mean damping rate is always less than the rate of a rectangular pulse with $f = f_c$. From this one could expect that the maximal reduction of the amplitude of RRs should be stronger for the rectangular pulse. However, it is clearly seen from Fig. 5 that the maximal reduction is stronger for the Gaussian pulse. This is because here, the Gaussian pulse extends over a longer time interval than its rectangular counterpart (cf. Fig. 4). Thus, for the Gaussian pulse the longer lasting damping may overcompensate the reduced damping rate and lead to a more pronounced suppression of RRs. This also helps to explain why for high pulse areas the reduction of the RR amplitude is stronger for the Gaussian pulse. However, the reduced reappearance rate is mainly due to the smaller field strengths contained in the tails of the Gaussian pulse. In the limit of strong fields some of these components are close to f_c and experience a much stronger damping than the single field strength of a rectangular pulse. Applying even higher pulse areas does not eliminate these components from the frequency spectrum contained in the Gaussian pulse, and therefore, the undamping of RRs at high pulse areas is less pronounced. As the range of field strengths with likewise strong damping is wider at higher temperatures and for smaller dot sizes (cf. Fig. 2), the effects of different pulse shapes become more distinctive in this parameter region.

Let us now come to the case of sech-shaped pulses. As the hyperbolic secant distribution shares many properties with a Gaussian distribution, the differences in comparison with the rectangular pulse are similar. However, the hyperbolic secant shows a lower peak and heavier tails than a Gaussian distribution with the same FWHM. These differences are reflected in the RR scenario shown in the last column of Fig. 5. As the maximum of the distribution is smaller, the shift of the critical pulse area to higher values is larger than for a Gaussian pulse (cf. Fig. 6). In addition, the reappearance rate at strong fields is even more suppressed, as the tails containing field strengths for which the damping is stronger become more important. Therefore, the washing out of the reappearance is more pronounced and it will be more difficult to observe the

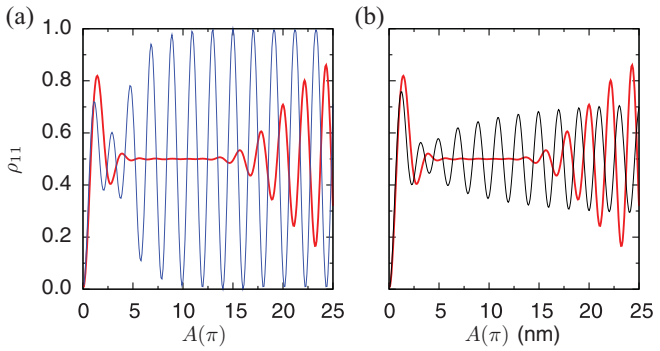

FIG. 7. (Color online) Quantum dot occupation as a function of the pulse area A at $T = 100$ K for a dot of $a = 5$ nm size. Comparison between a 20 ps lasting rectangular pulse (red, thick) with (a) a rectangular pulse of 5.4 ps duration (blue, thin) and (b) a Gaussian pulse of 5.4 ps duration (black, thin).

decay and reappearance phenomenon experimentally when using sech-shaped pulses.

So far, we discussed results comparing bell-shaped pulses with a FWHM of 5.4 ps with a 5.4 ps lasting rectangular pulse. We demonstrated that the undamping of RRs is most clearly visible for excitations with rectangular pulses, as the reappearance sets in earlier and shows a stronger reappearance rate. However, as already stated above, for a rectangular pulse of 5.4 ps duration, both bell-shaped pulses extend over a longer time interval than their rectangular counterpart. In contrast, all profiles are localized in the time interval given by the rectangular pulse if its duration is increased to 20 ps [cf. Fig. 4(a)]. To complete our discussion, in Fig. 7 we compare the Rabi rotation scenario for this longer rectangular pulse with results discussed so far, presenting calculations for a 5-nm-sized dot at $T = 100$ K.

Shown in Fig. 7(a) are RRs for both rectangular pulses. For the longer pulse, the critical pulse area A_c rises significantly and the reappearance rate is less. Note that for rectangular pulses, $f = A/\tau$, where τ denotes the pulse duration. Therefore, to reach $f = f_c$ or to excess this value in order to come into the undamping regime, for a longer pulse higher pulse areas have to be applied. Thus, both differences can be understood as a consequence of the resonant nature of the carrier-phonon coupling.

Comparing the 20 ps lasting rectangular pulse with the Gaussian pulse in Fig. 7(b), the reappearance rate for the Gaussian pulse is still less than for the rectangular pulse, which follows straightforwardly from the discussion above. However, here, the reappearance sets in earlier for the Gaussian pulse. This is due to the fact that the peak of the Gaussian pulse contains field strengths much higher than the constant field strength of the rectangular pulse [cf. Fig. 4(a)]. In addition, for small pulse areas, the damping is less for the Gaussian pulse. The latter can be explained by a closer look on the dependence of the damping rate on the field strength as presented in Fig. 2. In the limit of weak fields the damping constant γ_d is a convex function, while it is concave at intermediate fields. One important property of convex functions is the validity of Jensen's inequality, stating in its simplest form that the mean after a convex transformation is more than or equal to the convex transformation of a mean. Let us now consider a pulse area corresponding to a mean field strength $f \ll f_c$, where f_c marks the critical field strength of a rectangular pulse. For a constant, rectangular pulse that contains only this field strength f, the exciton occupation will experience a certain damping. However, as the different field strengths contained within the Gaussian pulse enter the damping function, which is convex for small fields, the effective damping rate after the weighting, which is introduced by the Gaussian shape, is stronger. As both envelope functions are localized in the time interval given by the rectangular pulse, this directly translates into a stronger damping. Along similar lines, one can understand that the maximal reduction of the RR amplitude is less for a Gaussian pulse: In contrast to a rectangular pulse with $f = f_c$, a Gaussian pulse always contains less damped field strength, and therefore, the maximal damping is less. Even if this is trivial, it is related to the concavity of the damping rate at intermediate fields. We would like to stress that in this context, it is the dot size that defines, via the field-strength-dependent damping, the characterization of fields as weak, intermediate, or strong.

In the previous discussions we have seen that practically all dependencies of RRs on the pulse shape or length can be traced back to the dependence of the damping rate on the field strength, as shown in Fig. 2, and the corresponding consequences for excitations with pulses with different field strength composition. Thus, rectangular pulses containing only one field strength most directly translate the nonmonotonic dependence of the damping rate to the decay and reappearance of RRs. In contrast, pulses containing more than one field strength more or less smear out the undamping effect as seen in the representative examples of Gaussian or sech-shaped pulses. This argument also holds for pulse sequences. Indeed, we have performed additional calculations for rectangular double pulses. Double pulses or even more sophisticated pulse sequences are discussed in the context of control of decoherence in optically excited quantum dots[4,5,31] but also to enhance the charge transfer in double dot structures.[32–35] In fact, our calculations for double pulses having the same total length as the single rectangular pulses considered so far show a slightly changed damping, but there is practically no effect on the visibility of the decay and reappearance.

IV. CONCLUSIONS

We have analyzed the dependence of the phonon-induced damping in an optically driven QD on the dot size and the shape of externally applied laser pulses, concentrating on pure dephasing processes. As demonstrated above, the choice of both parameters considerably affects the field-strength-dependent dynamics. For smaller dots the exciton-phonon coupling is effectively enhanced and the system experiences a much stronger damping, whereby the pulse area with maximal dephasing is shifted to higher values. However, we found that in the limit of weak fields, which may be most convenient in experimental investigations, the damping is approximately independent on the dot size. This is an opposite trend compared with the renormalization of the Rabi frequency, which in the weak-field limit shows a pronounced temperature-dependent decrease for smaller widths of the electronic confinement and leads to a normalized period of ROs which can exceed the

phonon-free period by more than a factor of 2. A comparison between the decay and reappearance of RRs in the cases of rectangular and Gaussian or sech-shaped pulses revealed marked differences. For a rectangular pulse, whose length coincides with the FWHM of the bell-shaped pulses, the reappearance sets in for smaller pulse areas and the reappearance rate is stronger. Thus, the decay and reappearance is most pronounced for rectangular profiles.

We believe that our studies may inspire future experimental investigations. Our results can be used as a guideline to choose proper parameters in order to observe the decay and reappearance of RRs, resulting from the non-Markovian nature of pure dephasing, experimentally.

ACKNOWLEDGMENTS

M.G. and M.D.C. acknowledge financial support by the Studienstiftung des Deutschen Volkes and the Alexander von Humboldt Foundation, respectively.

*martin.glaessl@uni-bayreuth.de

[1] M. A. Nielsen and I. Chuang, *Quantum Computation and Quantum Information* (Cambridge University Press, England, 2000).
[2] E. Biolatti, R. C. Iotti, P. Zanardi, and F. Rossi, Phys. Rev. Lett. **85**, 5647 (2000).
[3] F. Troiani, U. Hohenester, and E. Molinari, Phys. Rev. B **62**, R2263 (2000).
[4] P. Chen, C. Piermarocchi, and L. J. Sham, Phys. Rev. Lett. **87**, 067401 (2001).
[5] C. Piermarocchi, P. Chen, Y. S. Dale, and L. J. Sham, Phys. Rev. B **65**, 075307 (2002).
[6] X. Q. Li, Y. W. Wu, D. Steel, D. Gammon, T. H. Stievater, D. S. Katzer, D. Park, C. Piermarocchi, and L. J. Sham, Science **301**, 809 (2003).
[7] S. Stufler, P. Ester, A. Zrenner, and M. Bichler, Phys. Rev. B **72**, 121301(R) (2005).
[8] Q. Q. Wang, A. Muller, P. Bianucci, E. Rossi, Q. K. Xue, T. Takagahara, C. Piermarocchi, A. H. MacDonald, and C. K. Shih, Phys. Rev. B **72**, 035306 (2005).
[9] A. J. Ramsay, A. V. Gopal, E. M. Gauger, A. Nazir, B. W. Lovett, A. M. Fox, and M. S. Skolnick, Phys. Rev. Lett. **104**, 017402 (2010).
[10] A. J. Ramsay, T. M. Godden, S. J. Boyle, E. M. Gauger, A. Nazir, B. W. Lovett, A. M. Fox, and M. S. Skolnick, Phys. Rev. Lett. **105**, 177402 (2010).
[11] A. Vagov, V. M. Axt, and T. Kuhn, Phys. Rev. B **66**, 165312 (2002).
[12] A. Vagov, V. M. Axt, T. Kuhn, W. Langbein, P. Borri, and U. Woggon, Phys. Rev. B **70**, 201305(R) (2004).
[13] T. Takagahara, Phys. Rev. B **60**, 2638 (1999).
[14] J. Förstner, C. Weber, J. Danckwerts, and A. Knorr, Phys. Rev. Lett. **91**, 127401 (2003).
[15] A. Vagov, M. D. Croitoru, V. M. Axt, T. Kuhn, and F. M. Peeters, Phys. Status Solidi B **243**, 2233 (2006).
[16] A. Krügel, V. M. Axt, T. Kuhn, P. Machnikowski, and A. Vagov, Appl. Phys. B **81**, 897 (2005).
[17] P. Borri, W. Langbein, S. Schneider, U. Woggon, R. L. Sellin, D. Ouyang, and D. Bimberg, Phys. Rev. Lett. **87**, 157401 (2001).
[18] B. Krummheuer, V. M. Axt, and T. Kuhn, Phys. Rev. B **65**, 195313 (2002).
[19] A. Vagov, M. D. Croitoru, M. Glässl, V. M. Axt, and T. Kuhn, Phys. Rev. B **83**, 094303 (2011).
[20] N. Makri and D. Makarov, J. Chem. Phys. **102**, 4600 (1995).
[21] N. Makri and D. Makarov, J. Chem. Phys. **102**, 4611 (1995).
[22] M. Thorwart, J. Eckel, and E. R. Mucciolo, Phys. Rev. B **72**, 235320 (2005).
[23] E. Sim, J. Chem. Phys. **115**, 4450 (2001).
[24] A. Vagov, M. D. Croitoru, V. M. Axt, T. Kuhn, and F. M. Peeters, Phys. Rev. Lett. **98**, 227403 (2007).
[25] P. Machnikowski and L. Jacak, Phys. Rev. B **69**, 193302 (2004).
[26] E. T. Jaynes and F. W. Cummings, Proc. IEEE **51**, 89 (1963).
[27] G. D. Mahan, *Many-Particle Physics*, 2nd ed. (Plenum, New York, 1990) .
[28] V. M. Axt, T. Kuhn, A. Vagov, and F. M. Peeters, Phys. Rev. B **72**, 125309 (2005).
[29] A. Vagov, M. D. Croitoru, V. M. Axt, P. Machnikowski, and T. Kuhn, Phys. Status Solidi B **248**, 839842 (2011).
[30] A. M. Weiner, Prog. Quantum Electron. **19**, 161 (1995).
[31] V. M. Axt, P. Machnikowski, and T. Kuhn, Phys. Rev. B **71**, 155305 (2005).
[32] O. Speer, M. E. Garcia, and K. H. Bennemann, Phys. Rev. B **62**, 2630 (2000).
[33] I. Grigorenko, O. Speer, and M. E. Garcia, Phys. Rev. B **65**, 235309 (2002).
[34] S. G. Kosionis, A. F. Terzis, and E. Paspalakis, Phys. Rev. B **75**, 193305 (2007).
[35] E. Räsänen, A. Castro, J. Werschnik, A. Rubio, and E. K. U. Gross, Phys. Rev. B **77**, 085324 (2008).